



# One-pot synthesis of 4,4-(arylmethylene)-bis-(3-methyl-1-phenyl-1H-pyrazol-5-ols) catalyzed by Brønsted acidic ionic liquid supported on nanoporous Na<sup>+</sup>-montmorillonite



Farhad Shirini\*, Mohadeseh Seddighi, Masoumeh Mazloumi, Masoumeh Makhsous, Masoumeh Abedini

Department of Chemistry, College of Science, University of Guilan, Rasht 41335, Post Box: 1914, Islamic Republic of Iran

## ARTICLE INFO

Available online xxxx

### Keywords:

Montmorillonite  
Immobilization of ionic liquid  
3-Methyl-1-phenyl-5-pyrazolone  
4,4-(Arylmethylene)-bis-(1H-pyrazol-5-ols)

## ABSTRACT

Na<sup>+</sup>-MMT-[pmim]HSO<sub>4</sub>, obtained from the immobilization of 1-methyl-3-(trimethoxysilylpropyl)-imidazolium hydrogen sulfate ionic liquid on nanoporous Na<sup>+</sup>-montmorillonite, was used as catalyst for the simple and efficient synthesis of 4,4-(arylmethylene)-bis-(3-methyl-1-phenyl-1H-pyrazol-5-ol) derivatives via the one-pot condensation of phenyl hydrazine, ethyl acetoacetate and aldehydes. These reactions were performed at 80 °C under solvent free conditions with high yields in short reaction times. Low loading of the catalyst, simple experimental procedure and use of an inexpensive catalyst are some of advantages of the procedure. Also this catalyst can be reused several times without loss of its catalytic activity.

© 2015 Elsevier B.V. All rights reserved.

## 1. Introduction

Heterocyclic compounds are widely distributed in nature and are essential to life. Pyrazoles are important classes of heterocyclic compounds that occur widely in the pharmaceutical industry. For example, compounds containing 2,4-dihydro-3H-pyrazol-3-one structural motif, including 4,4-(arylmethylene)-bis-(1H-pyrazol-5-ols), have attracted an interest because they exhibit a wide range of biological activities such as antimalarial [1], antifungal [2], anti-inflammatory [3], antimicrobial [4], antinociceptive [5], analgesic [6], fungicide [7] and antitumor [8] activities. Additionally, they are applied as important intermediates in organic synthesis [9] and as bis-Schiff bases [10]. 4,4-(Arylmethylene)-bis-(1H-pyrazol-5-ols) were also used as pesticides [11], antiviral [12] and ligand [13]. The main synthetic method for the preparation of this type of compounds is based on the condensation of aldehydes with 3-methyl-1-phenyl-5-pyrazolone. Therefore, a variety of catalysts and reagents have been used to facilitate this reaction [13–22]. Although these procedures provide an improvement in the synthesis of these heterocyclic compounds, many of them suffer from disadvantages such as long reaction times, harsh reaction conditions, the need of excess amounts of the reagent, the use of organic solvents, the use of toxic reagents and non-recoverability of the catalyst. Therefore, introducing of simple, efficient and mild procedures with easily separable and reusable solid catalysts to overcome these problems is still in demand.

Over the last years, ionic liquids (ILs) have been extensively used in almost all application fields of chemistry such as organic and inorganic syntheses, catalysis, electrochemistry and chromatography. It is due to their remarkable properties such as non-flammability, negligible vapor pressure, wide liquid range and high thermal, chemical and electrochemical stability. However, their high cost, large consumption and difficult recovery and the separation of products cause limitations in the large-scale application of them. Furthermore, the ionic liquids (especially Brønsted acidic ionic liquids) have some degree of instability in the presence of air and moisture. Immobilization of the ionic liquids on the surface of a solid support is a useful way to combine the advantageous characteristics of ionic liquids and solid properties. In other words, the immobilized ionic liquids offer the additional features compared to the pure ionic liquids that facilitate the handling, separation and reuse procedures, and minimizing the amount of IL utilized in reactions [23].

In recent years, clays as nanostructured materials have been widely used in organic transformations as solid acid catalysts [24–27]. The main reasons for use of clays are the large specific surface area, chemical and mechanical stability, layered structure and high cation exchange capacity as well as accessibility, easy modification, cheapness and non-corrosiveness. One such clay is montmorillonite (MMT), which consists of two tetrahedral silicate sheets with a central aluminum octahedral sheet, exhibits a net negative charge on the lamellar surface and causes them to adsorb cations, such as Na<sup>+</sup> or Ca<sup>+</sup> for compensation. Layers of MMT have a thickness of about 1 nm and a length of 100 nm or a little more, so MMT is a structurally well-ordered nanoporous material.

\* Corresponding author.  
E-mail address: [shirini@guilan.ac.ir](mailto:shirini@guilan.ac.ir) (F. Shirini).

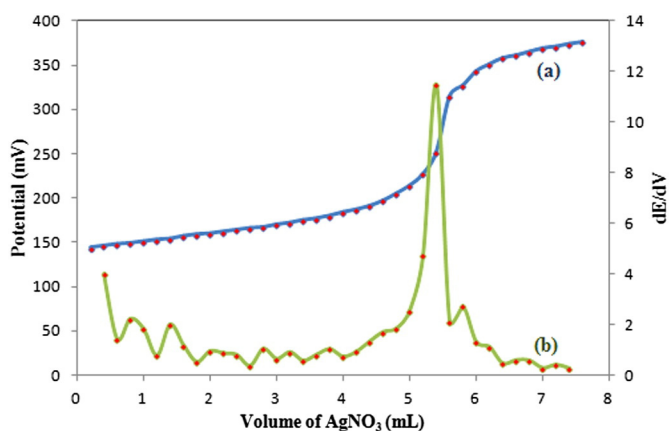


Fig. 1. Potentiometric titration and its first derivative curves of  $\text{Na}^+$ -MMT-[pmim]Cl with  $\text{AgNO}_3$ .

However, they require the cation exchange or surface modification to increase their active sites for better interaction with reactants.

## 2. Experimental

### 2.1. General

Chemicals were purchased from Fluka, Merck, and Aldrich chemical companies. All yields refer to the isolated products. Products were characterized by comparison of, their physical constants, IR and NMR spectroscopy with authentic samples and those reported in the literature. The purity determination of the substrate and reaction monitoring were accompanied by TLC on silica gel polygram SILG/UV 254 plates.

### 2.2. Preparation of 1-methyl-3-(trimethoxysilylpropyl)-imidazolium chloride ([pmim]Cl)

A mixture of 10 mmol of 1-methylimidazole and 10 mmol of (3-chloropropyl)trimethoxysilane was refluxed at  $90^\circ\text{C}$  for 30 h. Then, the reaction mixture was cooled down. The crude product was washed with  $\text{Et}_2\text{O}$  ( $2 \times 5$  mL) and dried under vacuum. The product as a slightly yellow viscous oil was obtained.

### 2.3. Preparation of 1-methyl-3-(trimethoxysilylpropyl)-imidazolium chloride supported on sodium montmorillonite ( $\text{Na}^+$ -MMT-[pmim]Cl)

1.2 g (4 mmol) of [pmim]Cl was dissolved in 25 mL of  $\text{CH}_2\text{Cl}_2$  and treated with 2 g of sodium montmorillonite. The reaction mixture was refluxed with stirring for 3 days. Then, the reaction mixture was cooled to room temperature, the solid was isolated by filtration and washed with 20 mL of boiling dichloromethane to remove the unreacted ionic liquid. In the next step, the material was dried to obtain MMT-[pmim]Cl. The amount of chloride in MMT-[pmim]Cl was determined by potentiometric titration methods [28]. For this purpose, 0.5 g of MMT-[pmim]Cl in 50 mL water was titrated with 0.1 M  $\text{AgNO}_3$ . As shown in Fig. 1, the change happened at 5.1 mL of consumed  $\text{AgNO}_3$ . On the basis of these studies it can be concluded that  $\text{Na}^+$ -MMT-[pmim]Cl has 1.02 mmol of  $\text{Cl}^-$  per gram of this reagent.

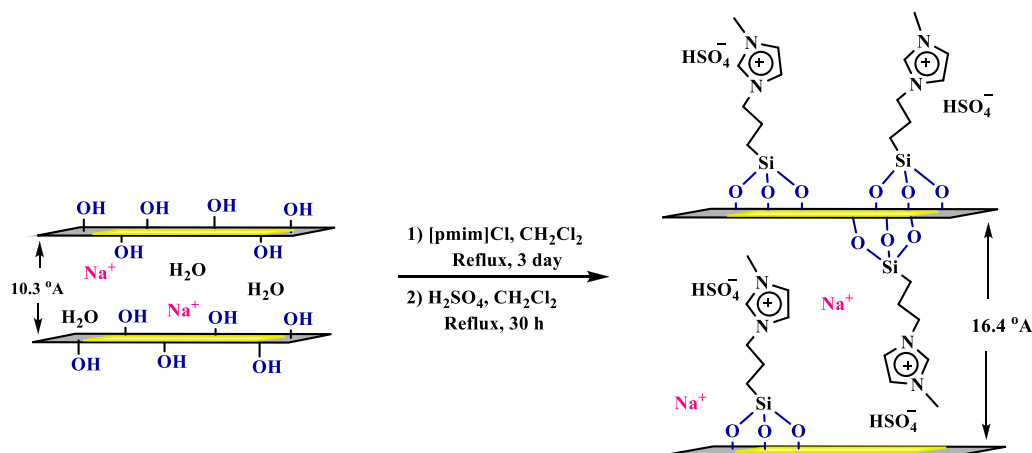
### 2.4. Preparation of 1-methyl-3-(trimethoxysilylpropyl)-imidazolium hydrogen sulfate supported on sodium montmorillonite ( $\text{Na}^+$ -MMT-[pmim]HSO<sub>4</sub>)

3 g of  $\text{Na}^+$ -MMT-[pmim]Cl was suspended in 20 mL of dry  $\text{CH}_2\text{Cl}_2$ . Under vigorous stirring and in an ice bath ( $0^\circ\text{C}$ ) 3 mmol of concentrated  $\text{H}_2\text{SO}_4$  (97%) was added dropwise to this mixture. The mixture was then warmed to room temperature and heated under reflux for 30 h. When the formed HCl was completely distilled off the solution was cooled and  $\text{CH}_2\text{Cl}_2$  was removed under vacuum to afford  $\text{Na}^+$ -MMT-[pmim]HSO<sub>4</sub> as the product (Scheme 1).

### 2.5. Catalyst characterization

#### 2.5.1. Instrumentation

The FT-IR spectra were run on a VERTEX 70 Bruker company (Germany). Thermogravimetric analyses (TGA) were performed on Polymer Laboratories PL-TGA thermal analysis instrument (England). Samples were heated from 25 to  $600^\circ\text{C}$  at ramp  $10^\circ\text{C}/\text{min}$  under  $\text{N}_2$  atmosphere. Scanning electron microphotographs (SEM) were obtained on a SEM-Philips XL30. X-ray diffraction (XRD) measurements were performed at room temperature on diffractometer Model XRD 6000, PHILIPS Xpert pro using  $\text{Co-K}\alpha$  radiation ( $K = 1.7890 \text{ \AA}$ ) with the beam voltage and a beam current of 40 kV and 30 mA, respectively. Transmission electron microscopy (TEM) analysis was performed on a Philips model CM 30 instrument.



Scheme 1. Preparation of the acidic ionic liquid immobilized on  $\text{Na}^+$ -MMT ( $\text{Na}^+$ -MMT-[pmim]HSO<sub>4</sub>).

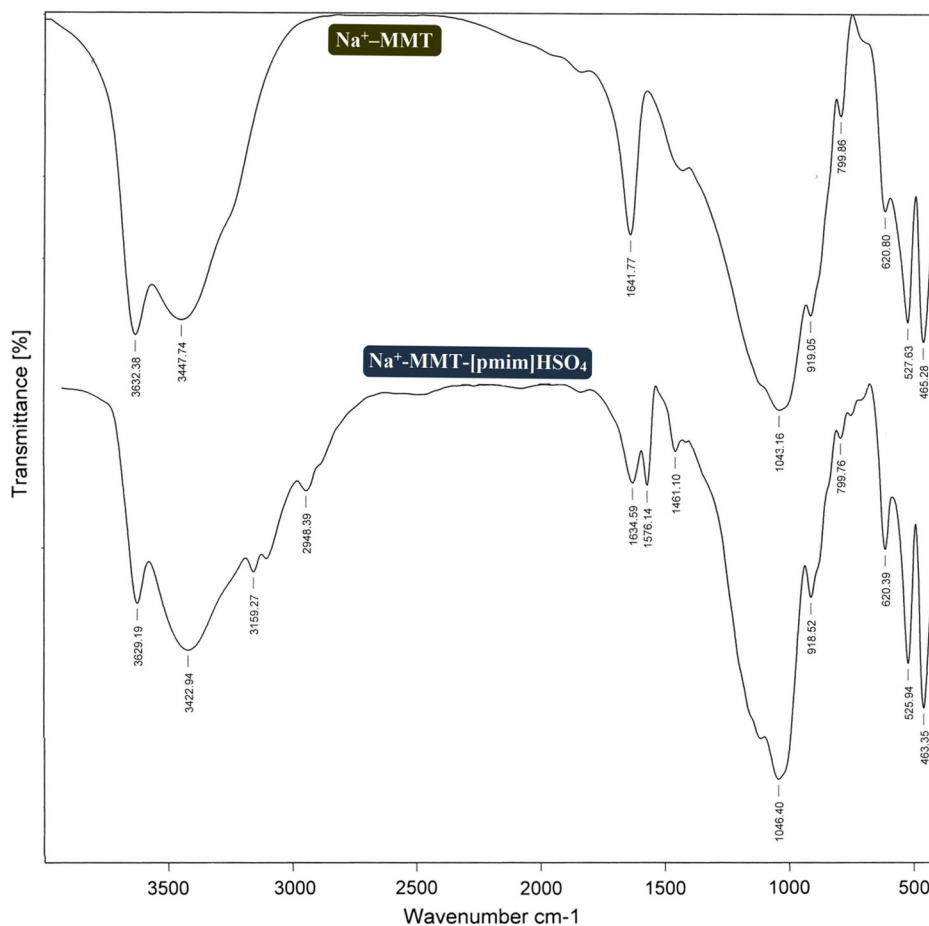


Fig. 2. FT-IR spectra of Na<sup>+</sup>-MMT and Na<sup>+</sup>-MMT-[pmim]HSO<sub>4</sub>.

### 2.5.2. IR analysis

The infrared spectra of Na<sup>+</sup>-MMT and Na<sup>+</sup>-MMT-[pmim]HSO<sub>4</sub> are presented in Fig. 2. The FT-IR spectrum of pristine clay displays the peak at 3632 cm<sup>-1</sup> that can be attributed to the OH units in Na<sup>+</sup>-MMT. The peaks at 3423 and 1641 cm<sup>-1</sup> correspond to the -OH stretching vibration of free H<sub>2</sub>O onto the Na<sup>+</sup>-MMT structure and the bands at 1043 and 919 cm<sup>-1</sup> can be collectively attributed to Si-O stretching vibrations [27,29].

The Na<sup>+</sup>-MMT-[pmim]HSO<sub>4</sub> is also characterized on the basis of its FT-IR (Fig. 2). The peaks at 1576 and 1635 cm<sup>-1</sup> can be assigned to C=N and C=C bands of the attached imidazolium ring. Additional bands at 3159, 2948 and 1461 cm<sup>-1</sup> were due to C-H stretching and deformation vibrations, confirming the functionalization of the material

with the ionic liquid [30]. The absorption of the S=O asymmetric stretching mode appeared at 1170 cm<sup>-1</sup> and its symmetric stretching mode lie in 1060 cm<sup>-1</sup>, so the broad band around 1046 cm<sup>-1</sup> can be assigned to the stretching modes of Si-O and S=O bands which are overlapped together. The S-O stretching modes of sulfuric acid functional group lie around 620 and 890 cm<sup>-1</sup> proving the successful preparation of the catalyst [31].

### 2.5.3. SEM analysis

The samples of Na<sup>+</sup>-MMT and Na<sup>+</sup>-MMT-[pmim]HSO<sub>4</sub> were also analyzed by scanning electron microscopy (SEM) for determining the size distribution, particle shape and surface morphology, as represented in Fig. 3. The pictures show that the original structure of Na<sup>+</sup>-MMT is

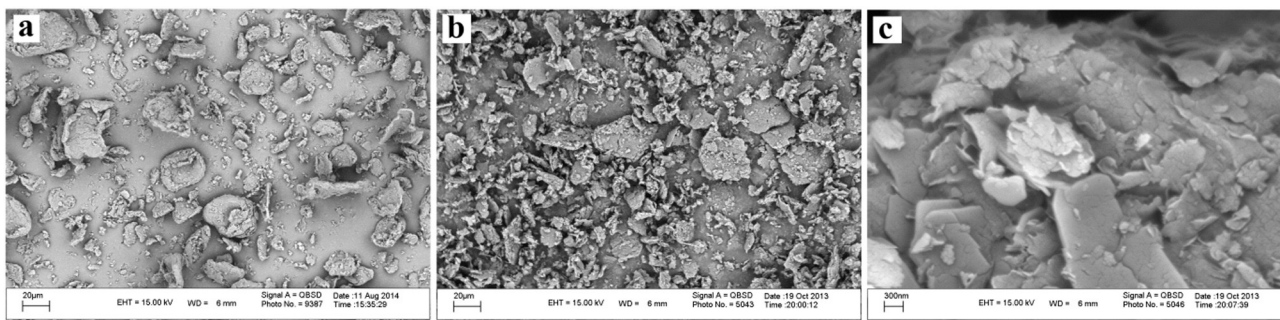


Fig. 3. SEM images of Na<sup>+</sup>-MMT (a) and Na<sup>+</sup>-MMT-[pmim]HSO<sub>4</sub> (b,c).

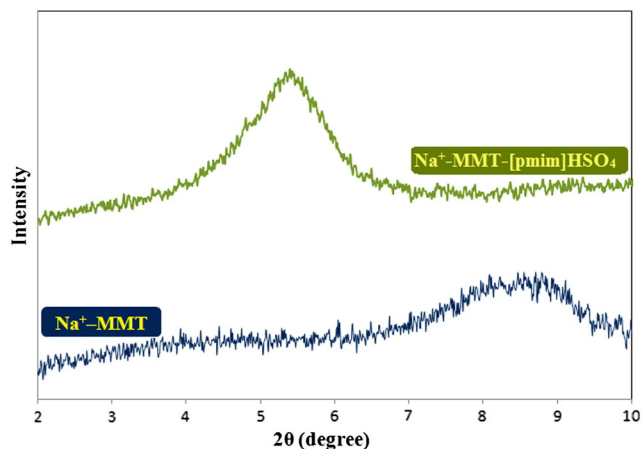


Fig. 4. XRD patterns of  $\text{Na}^+$ -MMT in comparison with  $\text{Na}^+$ -MMT-[pmim] $\text{HSO}_4$ .

changed and the particles are clearly less stacked in the intercalated clays. This opening of the layers suggests that the interlayer space may be occupied by the organic molecules. These images also show that  $\text{Na}^+$ -MMT-[pmim] $\text{HSO}_4$  appears as particles with irregular plate-like shapes.

#### 2.5.4. Powder X-ray diffraction

Fig. 4 represents the X-ray diffractograms of samples, containing sodium montmorillonite and  $\text{Na}^+$ -MMT-[pmim] $\text{HSO}_4$  to demonstrate the expansion of the montmorillonite layers. The calculated basal spacing for the  $\text{Na}^+$ -MMT is 10.3 Å with  $2\theta = 8.6^\circ$  and for  $\text{Na}^+$ -MMT-[pmim] $\text{HSO}_4$  is 16.4 Å. The basal spacing of the ionic liquid anchored

sodium montmorillonite is obviously bigger than that of  $\text{Na}^+$ -MMT, indicating that the ionic liquid has been intercalated into montmorillonite interlayer spaces [32]. This increase in the basal spacing can lead to the better interaction between the reactants in the acid catalysis reactions, in comparison with the montmorillonite. From the d-spacing of  $\text{Na}^+$ -MMT-[pmim] $\text{HSO}_4$  the existence of one molecule of ionic liquid between the clay layers could be estimated [33].

#### 2.5.5. Transmission electron microscopy (TEM)

In addition to XRD, the TEM was also applied to visualize the spatial morphology of  $\text{Na}^+$ -MMT-[pmim] $\text{HSO}_4$ , as shown in Fig. 5. The dark line represents the intersection silicate layers of MMT while the gray background represents the interlayer organic compounds. The results indicated that after incorporation of ionic liquid with MMT the intercalated nanostructure was obtained. Furthermore, clusters or agglomerated clay platelets could be seen in these images.

#### 2.5.6. Surface area and pore distribution measurements

$\text{N}_2$  adsorption–desorption measurements based on BET and BJH methods were performed to obtain more information about the catalyst. The adsorption–desorption isotherm of  $\text{Na}^+$ -MMT and  $\text{Na}^+$ -MMT-[pmim] $\text{HSO}_4$  is shown in Fig. 6a. Both samples exhibited type V isotherm with  $\text{H}_3$  hysteresis loop categories according to the literature [34], which indicates the micro and mesopore structures of samples with slit-like pores [35]. These results also prove that the textural properties of  $\text{Na}^+$ -MMT were substantially maintained over immobilization of ionic liquid. BET surface areas, the total pore volumes ( $V_t$ ),  $V_{\text{microp}}$  (estimated by t-plot method) and pore diameters for  $\text{Na}^+$ -MMT and  $\text{Na}^+$ -MMT-[pmim] $\text{HSO}_4$  were presented in Table 1. A decrease in BET surface area from  $\text{Na}^+$ -MMT (156.0  $\text{m}^2/\text{g}$ ) to  $\text{Na}^+$ -MMT-[pmim] $\text{HSO}_4$  (133.4  $\text{m}^2/\text{g}$ ) was indicated that the ionic liquid may be successfully

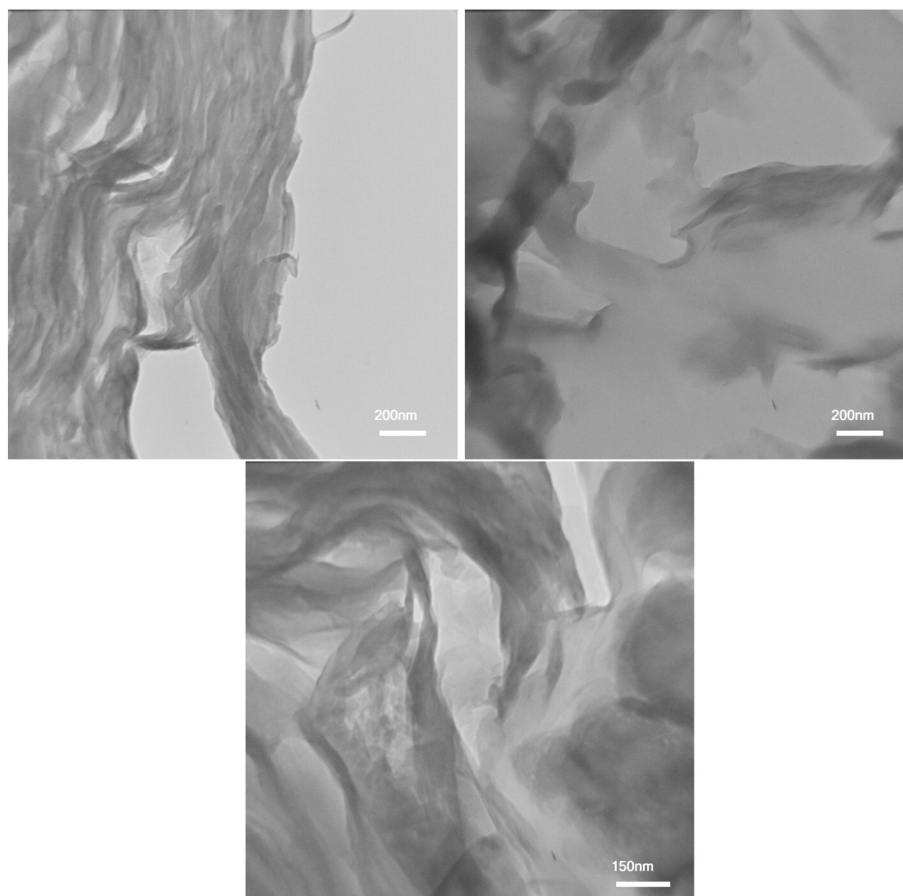


Fig. 5. TEM images of  $\text{Na}^+$ -MMT-[pmim] $\text{HSO}_4$ .

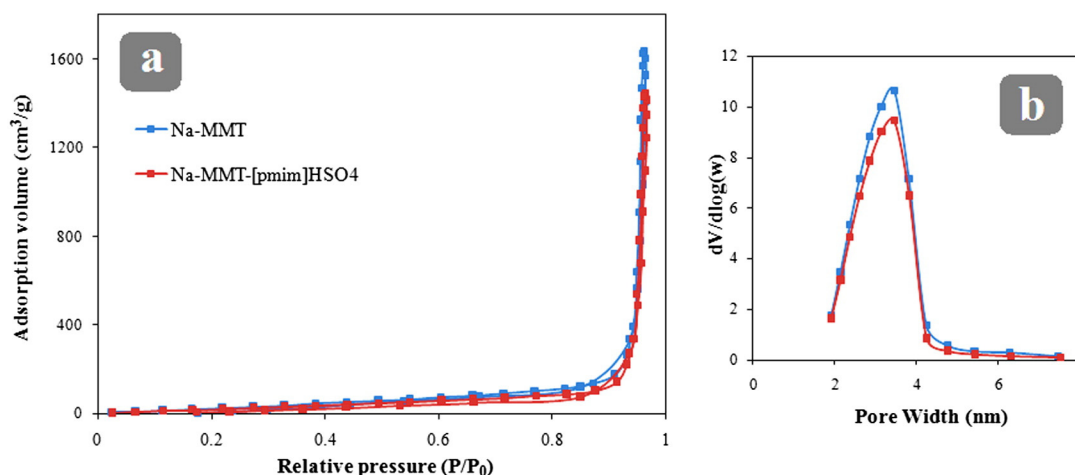


Fig. 6. The  $N_2$  adsorption–desorption isotherm (a), and pore size distribution (b) of  $Na^+$ -MMT and  $Na^+$ -MMT-[pmim]HSO<sub>4</sub>.

Table 1

Pore structure parameters of  $Na^+$ -MMT-[pmim]HSO<sub>4</sub> derived from the  $N_2$  adsorption–desorption isotherms.

Sample	$S_{BET}$ (m <sup>2</sup> /g)	$V_t$ (cm <sup>3</sup> /g)	$V_{microp}$ (cm <sup>3</sup> /g)	$D_{BJH}$ (nm)
$Na^+$ -MMT	156.0	56.44	0.0344	2.51
$Na^+$ -MMT-[pmim]HSO <sub>4</sub>	133.4	48.97	0.0275	2.50

intercalated to  $Na^+$ -MMT layers. The curves of pore size distribution evaluated from desorption data by utilizing the BJH model are also shown in Fig. 6b.

### 2.5.7. Thermal analysis

Thermogravimetric analysis (TGA) was performed for characterization of  $Na^+$ -MMT-[pmim]HSO<sub>4</sub> in comparison with sodium montmorillonite. Fig. 7 provides the TGA curve of pristine clay ( $Na^+$ -MMT) and catalyst. The TGA curve of  $Na^+$ -MMT displays a weight loss below 100 °C which is corresponding to the loss of the physically adsorbed water and interlayer H<sub>2</sub>O, also there is a slight weight loss in the range of 100–600 °C, possibly corresponding to dehydroxylation of sodium montmorillonite [27].

The TGA analysis of  $Na^+$ -MMT-[pmim]HSO<sub>4</sub> shows a completely different decomposition from  $Na^+$ -MMT. A small mass loss appeared at <100 °C because of the loss of water and a greater mass loss started from 270 °C can be attributed to the decomposition of the immobilized ionic liquid moieties anchored on the clay surface [36]. These results

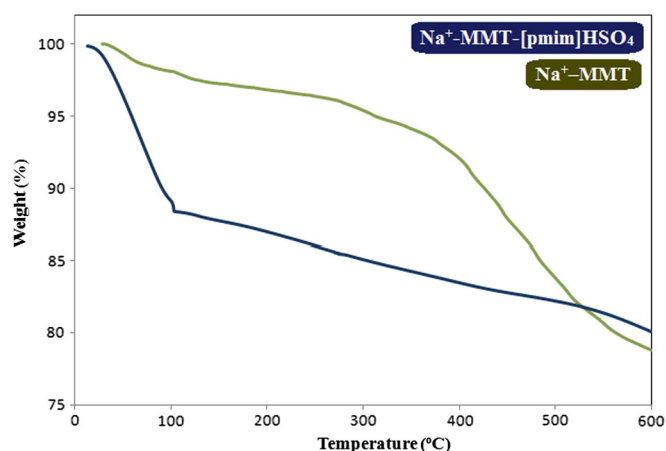


Fig. 7. TGA curves of  $Na^+$ -MMT and  $Na^+$ -MMT-[pmim]HSO<sub>4</sub>.

indicate that the immobilized acid catalyst has great thermal stability and is apparently stable up to about 270 °C.

### 2.6. General procedure for the synthesis of 4,4-(arylmethylene)-bis-(3-methyl-1-phenyl-1H-pyrazol-5-ols) derivatives (2)

Phenyl hydrazine (2 mmol) was added to a mixture of  $Na^+$ -MMT-[pmim]HSO<sub>4</sub> (50 mg) and ethyl acetoacetate (2 mmol) at 100 °C and was stirred for 1 min. Then the aldehyde (1 mmol) was added and the resulting mixture was stirred for the appropriate time (Table 1). After completion of the reaction (monitored by TLC), EtOH (10 mL) was added and the catalyst was separated by filtration. Then water was added and the precipitated product was separated by filtration in high purity.

**3-Methyl-1-phenyl-5-pyrazolone (1):** <sup>1</sup>H NMR (DMSO-d<sub>6</sub>, 400 MHz):  $\delta$  = 2.38 (3H, s, CH<sub>3</sub>), 3.36 (2H, s, CH<sub>2</sub>), 7.35 (1H, t,  $J$  = 7.6 Hz), 7.52 (2H, t,  $J$  = 8 Hz), 7.85 (2H, d,  $J$  = 8.0 Hz) ppm; <sup>13</sup>C NMR (DMSO-d<sub>6</sub>, 100 Mz):  $\delta$  = 13.14, 109.37, 121.29, 127.12, 129.55, 137.68, 140.97, 154.00, 161.15.

**4,4-(2-Methylphenylmethylene)bis(3-methyl-1-phenyl-1H-pyrazol-5-ol):** <sup>1</sup>H NMR (DMSO-d<sub>6</sub>, 400 MHz):  $\delta$  = 2.29 (9H, s, CH<sub>3</sub>), 4.94 (1H, s, CH<sub>2</sub>), 7.10–7.15 (3H, m), 7.24 (2H, t,  $J$  = 7.0 Hz), 7.44 (4H, t,  $J$  = 8.0 Hz), 7.51 (1H, d,  $J$  = 7.0 Hz), 7.72 (4H, d,  $J$  = 8.0 Hz), 12.36 (1H, s), 13.43 (1H, s) ppm; <sup>13</sup>C NMR (DMSO-d<sub>6</sub>, 100 Mz):  $\delta$  = 12.35, 20.20, 31.85, 120.77, 125.93, 126.60, 128.50, 129.40, 130.93, 135.72, 140.34.

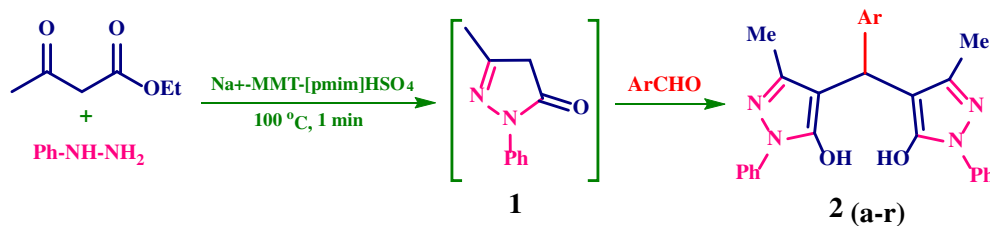
## 3. Results and discussion

On the basis of the information obtained from the studies on  $Na^+$ -MMT-[pmim]HSO<sub>4</sub>, we anticipated that this reagent can be used as an

Table 2

Optimization of the reaction conditions for the reaction of phenyl hydrazine, ethyl acetoacetate and 4-chlorobenzaldehyde catalyzed by  $Na^+$ -MMT-[pmim]HSO<sub>4</sub>.

Entry	Catalyst (mg)	Solvent	Temperature (°C)	Time (min)	Yield (%)
1	50	EtOH	Reflux	4 h	60
2	50	H <sub>2</sub> O	Reflux	4 h	90
3	50	CH <sub>3</sub> CN	Reflux	5 h	50
4	50	–	80	15	91
5	50	–	60	80	90
6	50	–	100	10	92
7	50	–	110	10	92
8	40	–	100	25	90
9	60	–	100	12	92



**Scheme 2.** One-pot synthesis of 4,4-(arylmethylene)-bis-(3-methyl-1-phenyl-1H-pyrazol-5-ols).

efficient solid acid catalyst for the promotion of the reactions which need the use of an acidic catalyst to speed-up. So we were interested to investigate the applicability of this reagent in the promotion of the synthesis of 4,4-(arylmethylene)-bis-(3-methyl-1-phenyl-1H-pyrazol-5-ols).

At first, we focused our attention to study the synthesis of 4,4-(arylmethylene)-bis-(3-methyl-1-phenyl-1H-pyrazol-5-ols). For optimization of the reaction conditions, the reaction between phenyl hydrazine, ethyl acetoacetate and 4-chlorobenzaldehyde to the corresponding product was selected as a model reaction and the various conditions including amount of the catalyst, solvent and temperature were examined (Table 2). For choosing the reaction media, different solvents such as EtOH, H<sub>2</sub>O, CH<sub>3</sub>CN and solvent-free conditions were used and the best results were obtained in the absence of solvent, probably due to the increase in the concentration and also increase in the effective contacts of the reactants. Then more experiments were performed and observed that 50 mg of Na<sup>+</sup>-MMT-[pmim]HSO<sub>4</sub> was the optimal catalyst loading for this reaction, and higher catalyst loading did not improve the yield of the product to a greater extent. Finally the optimal reaction condition for this reaction was obtained using 50 mg of Na<sup>+</sup>-MMT-[pmim]HSO<sub>4</sub> at 100 °C under solvent free conditions (Scheme 2).

After optimization of the reaction conditions and in order to establish the effectiveness and the acceptability of the method, we explored the protocol with a variety of simple readily available substrates under the optimal conditions. The results were presented in Table 3. It was observed that under similar conditions, a wide range of aromatic aldehydes containing electron-withdrawing as well as electron-donating groups such as Cl, Br, F, CH<sub>3</sub>, OCH<sub>3</sub>, NO<sub>2</sub>, SCH<sub>3</sub> and CN in the ortho, meta, and para positions of the benzene ring easily converted to the

corresponding 4,4-(arylmethylene)-bis-(3-methyl-1-phenyl-1H-pyrazol-5-ols) in short reaction times with good to excellent isolated yields (Table 3, entries 1–14). Furthermore, 2-naphthaldehyde as a polycyclic aromatic aldehyde also provided the desired product in very good yield (Table 3, entry 15). This method was also found to be useful for the usage of dialdehydes. In this reaction, 4 equivalents of 3-methyl-1-phenyl-5-pyrazolone successfully condensed with 1 equivalent of terephthalaldehyde and di-4,4-(phenylmethylene)-bis-(3-methyl-1-phenyl-1H-pyrazol-5-ol) was obtained in high yield at short time that shows the practical synthetic efficiency of this reaction (Table 3, entry 16).

In order to show the efficiency of the presented method, we have compared our result obtained for the synthesis of 4,4-(4-chlorophenylmethylene)-bis-(3-methyl-1-phenyl-1H-pyrazol-5-ol) catalyzed by Na<sup>+</sup>-MMT-[pmim]HSO<sub>4</sub> with some of the other results reported in the literature (Table 4). This method avoids disadvantages of the other procedures such as long reaction times, toxic reagents, high temperature, organic solvents, excess reagents and low yield. It is also important to note that the reported procedures for the synthesis of 4,4-(arylmethylene)-bis-(3-methyl-1-phenyl-1H-pyrazol-5-ols) are based on the condensation of aldehydes with 3-methyl-1-phenyl-5-pyrazolone, while our method is based on the one-pot condensation of phenyl hydrazine, ethyl acetoacetate and aldehydes. On the basis of the obtained results we believe that the reaction proceed via the in-situ generation of 3-methyl-1-phenyl-5-pyrazolone (1) which in reaction with aldehydes produces the requested products. This comparison also clarifies an important point about the catalyst. As it can be seen, Na<sup>+</sup>-MMT and Na<sup>+</sup>-MMT-[pmim]Cl are also able to catalyze this type of reactions but in longer reaction times rather than Na<sup>+</sup>-MMT-

**Table 3**  
Preparation of pyrano[2,3-d]pyrimidinone derivatives catalyzed by Na<sup>+</sup>-MMT-[pmim]HSO<sub>4</sub>.

Entry	Ar	Product	Time (min)	Yield (%)	Melting point (°C)	
					Found	Reported
1	C <sub>6</sub> H <sub>5</sub> -	<b>2a</b>	14	91	167–169	169–171 [20]
2	2-ClC <sub>6</sub> H <sub>4</sub> -	<b>2b</b>	14	89	240–242	236–237 [14]
3	4-ClC <sub>6</sub> H <sub>4</sub> -	<b>2c</b>	10	92	207–209	207–209 [14]
4	4-BrC <sub>6</sub> H <sub>4</sub> -	<b>2d</b>	10	91	210–212	215 [37]
5	4-FC <sub>6</sub> H <sub>4</sub> -	<b>2e</b>	10	91	188–190	180–182 [20]
6	2-CH <sub>3</sub> C <sub>6</sub> H <sub>5</sub> -	<b>2f</b>	20	90	230–232	-
7	2-CH <sub>3</sub> OC <sub>6</sub> H <sub>5</sub> -	<b>2g</b>	30	87	213–215	210–213 [16]
8	3-CH <sub>3</sub> OC <sub>6</sub> H <sub>5</sub> -	<b>2h</b>	30	89	192–194	193–194 [37]
9	4-CH <sub>3</sub> OC <sub>6</sub> H <sub>5</sub> -	<b>2i</b>	20	90	173–175	172–174 [16]
10	2-NO <sub>2</sub> C <sub>6</sub> H <sub>4</sub> -	<b>2j</b>	45	89	228–230	221–222 [16]
11	3-NO <sub>2</sub> C <sub>6</sub> H <sub>4</sub> -	<b>2k</b>	10	90	164–166	152–154 [20]
12	4-NO <sub>2</sub> C <sub>6</sub> H <sub>4</sub> -	<b>2l</b>	15	91	226–228	225–227 [15]
13	4-CH <sub>3</sub> SC <sub>6</sub> H <sub>5</sub> -	<b>2m</b>	25	90	204–206	201–203 [15]
14	4-CNC <sub>6</sub> H <sub>5</sub> -	<b>2n</b>	25	93	208–210	206–208 [20]
15	2-Naphthyl-	<b>2o</b>	25	91	202–204	206–208 [18]
16		<b>2q</b>	70	84	216–218	209–212 [38]

**Table 4**

Comparison of the result obtained from the synthesis 4,4'-(4-chlorophenylmethylene)bis(3-methyl-1-phenyl-1H-pyrazol-5-ol) in the presence of Na<sup>+</sup>-MMT-[pmim]HSO<sub>4</sub> with those obtained using some of the other catalysts.

Entry	Catalyst (loading)	Reaction conditions	Time (min)	Yield (%)	Ref.
1	SDS (5 mol%)	Reflux/H <sub>2</sub> O	1 h	91.5	[14]
2	Silica-bonded S-sulfonic acid (100 mg)	Reflux/EtOH	50	90	[15]
3	[HMIM]HSO <sub>4</sub> (10 mol%)	EtOH, US, r.t.	45	90	[16]
4	PEG-SO <sub>3</sub> H (1.5 mol%)	Reflux/H <sub>2</sub> O	30	94	[17]
5	Silica Sulfuric Acid (80 mg)	70 °C/EtOH:H <sub>2</sub> O	70	90	[18]
6	SASPSPE (100 mg)	Reflux/EtOH	2.2 h	85	[19]
7	[P4VPy-BuSO <sub>3</sub> H]HSO <sub>4</sub> (10 mol%)	Reflux/EtOH	50	95	[21]
8	Na <sup>+</sup> -MMT (50 mg)	100 °C/solvent free	45	90	This work
9	Na <sup>+</sup> -MMT-[pmim]Cl(50 mg)	100 °C/solvent free	18	92	This work
10	[pmim]HSO <sub>4</sub> (5 mol%)	100 °C/solvent free	30	Mixture	This work
11	Na <sup>+</sup> -MMT-[pmim]HSO <sub>4</sub> (50 mg, 5 mol%)	100 °C/solvent free	10	92	This work

[pmim]HSO<sub>4</sub>, and the mixture of products were obtained in the presence of [pmim]HSO<sub>4</sub> as catalyst. These results give clear evidence to confirm the important role of the covalently bounded ionic liquid and also HSO<sub>4</sub><sup>-</sup> group in the catalyst to obtain the best performance.

To check the reusability of the catalyst, the reaction of phenyl hydrazine, ethyl acetoacetate and 4-chlorobenzaldehyde under the optimized reaction conditions was studied again. When the reaction was completed, ethanol was added and the catalyst was separated by filtration. The recovered catalyst was washed with ethanol, dried and reused for the same reaction. This process was carried out over eight runs and all reactions led to the desired products without significant changes in terms of the reaction time and yield which clearly demonstrates practical recyclability of this catalyst (Fig. 8).

#### 4. Conclusion

In conclusion, in this study we have introduced Na<sup>+</sup>-MMT-[pmim]HSO<sub>4</sub> as a highly powerful supported acidic ionic liquid for the simple and efficient synthesis of 4,4'-(arylmethylene)-bis-(3-methyl-1-phenyl-1H-pyrazol-5-ols). The obtained results show that the catalytic activity of Na<sup>+</sup>-MMT-[pmim]HSO<sub>4</sub> is convincingly superior to other reported procedures in the terms of reaction times and yields. Lower loading of the catalyst, simple experimental procedure, and use of inexpensive and reusable catalyst are other advantages of the procedure. Furthermore, this process avoids problems associated with organic solvent and liquid acid use, which makes it a useful and attractive strategy in view of economic and environmental advantages. Further work to explore this catalyst in other organic transformations is in progress.

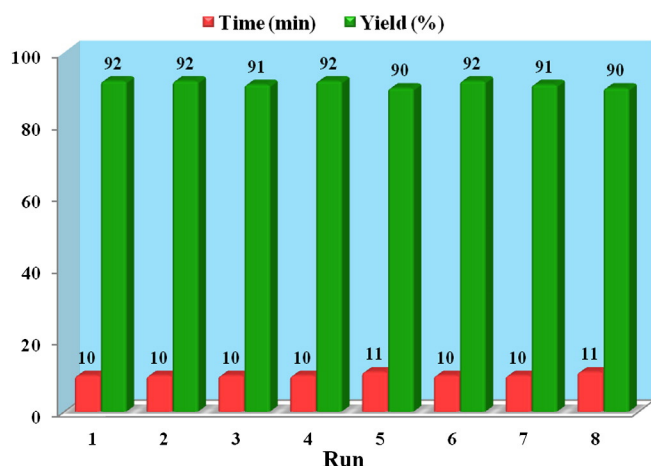


Fig. 8. Reusability of the catalyst.

#### Acknowledgments

We are thankful to the University of Guilan Research Council for the partial support of this work.

#### References

- [1] B.N. Acharya, D. Saraswat, M. Tiwari, A.K. Shrivastava, R. Ghorpade, S. Bapna, M.P. Kaushik, *Eur. J. Med. Chem.* 45 (2010) 430.
- [2] M. Kidwai, R.J. Mohan, *Korean Chem. Soc.* 48 (2004) 177.
- [3] Sugiura, S. Ohno, O. Ohtani, K. Izumi, T. Kitamikado, H. Asai, K. Kato, M. Hori, H. Fujimura, *J. Med. Chem.* 20 (1997) 80.
- [4] H. Bayrak, A. Demirbas, N. Demirbas, S.A. Karaoglu, *Eur. J. Med. Chem.* 45 (2010) 4726.
- [5] K.H. Carlsson, *I. Jurna, Naunyn Schmiedeberg's Arch. Pharmacol.* 335 (1987) 154.
- [6] G. Mariappan, P.B. Saha, L. Sutharson, A. Haldar, *Indian J. Chem. B* 49 (2010) 1671.
- [7] R.K. Tewari, R.K. Mishra, S.K. Srivastava, S.C. Bahel, *Pestic. Res. J.* 2 (1990) 24.
- [8] R.V. Antre, A. Cendilkumar, R. Nagarajan, D. Goli, R.J. Oswal, *J. Sci. Res.* 4 (2012) 183.
- [9] W.S. Hamama, *Synth. Commun.* 31 (2001) 1335.
- [10] T. Ren, S. Liu, G. Li, J. Zhang, J. Guo, W. Li, L. Yang, *Spectrochim. Acta A* 97 (2012) 167.
- [11] M. Londershausen, *Pestic. Sci.* 48 (1996) 269.
- [12] K. Sujatha, G. Shanthi, N.P. Selvam, S. Manoharan, P.T. Perumal, M. Rajendran, *Bioorg. Med. Chem. Lett.* 19 (2009) 4501.
- [13] M. Abbasi-Tarighat, E. Shahbazi, K. Niknam, *Food Chem.* 138 (2013) 991.
- [14] W. Wang, S. Wang, X. Qin, J. Li, *Synth. Commun.* 35 (2005) 1263.
- [15] K. Niknam, D. Saberi, M. Sadegheyan, A. Deris, *Tetrahedron Lett.* 51 (2010) 6928.
- [16] H. Zang, Q. Su, Y. Mo, B. Cheng, *Ultrason. Sonochem.* 18 (2011) 68.
- [17] A. Hasaninejad, M. Shekouhy, A. Zare, S.M.S.H. Ghattali, N. Golzar, *J. Iran. Chem. Soc.* 8 (2011) 411.
- [18] K. Niknam, S. Mirzaee, *Synth. Commun.* 41 (2011) 2403.
- [19] S. Tayabi, M. Baghernejad, D. Saberi, K. Niknam, *Chin. J. Catal.* 32 (2011) 1477.
- [20] N. Iravani, J. Albadi, H. Momtazan, M. Baghernejad, *J. Chin. Chem. Soc.* 60 (2013) 418.
- [21] K.P. Boroujeni, P. Shojaei, *Turk. J. Chem.* 37 (2013) 756.
- [22] A. Khazaei, F. Abbasi, A.R. Moosavi-Zare, *New J. Chem.* (2014) <http://dx.doi.org/10.1039/c4nj01079e>.
- [23] M.H. Valkenberg, C. deCastro, W.F. Hölderich, *Green Chem.* 4 (2002) 88.
- [24] S. Kantevari, S.V.N. Vuppapapati, L. Nagarapu, *Catal. Commun.* 8 (2007) 1857.
- [25] J.S. Yadav, B.V.S. Reddy, B. Eeshwaraiiah, M. Srinivas, *Tetrahedron* 60 (2004) 1767.
- [26] B.S. Kumar, A. Dhakshinamoorthy, K. Pitchumani, *Catal. Sci. Technol.* 4 (2014) 2378.
- [27] F. Shirini, M. Mamaghani, S.V. Atghia, *Catal. Commun.* 12 (2011) 1088.
- [28] J. William, *Handbook of Anion Determination*, First ed. Butterworths-Heinemann Ltd, London, 1979. 416.
- [29] M.H. Baki, F. Shemirani, R. Khani, M. Bayat, *Anal. Methods* 6 (2014) 1875.
- [30] S. Safaei, I. Mohammadpoor-Baltork, A.R. Khosropour, M. Moghadam, S. Tangestaninejad, V. Mirkhani, *Catal. Sci. Technol.* 3 (2013) 2717.
- [31] M.N. Sefat, D. Saberi, K. Niknam, *Catal. Lett.* 141 (2011) 1713.
- [32] K. Nagy, G. Biro, O. Berkesi, D. Benczedi, L. Ouali, I. Dékány, *Appl. Clay Sci.* 72 (2013) 155.
- [33] K. Wang, L. Wang, J. Wu, L. Chen, C. He, *Langmuir* 21 (2005) 3613.
- [34] J.B. Condon, *Surface Area and Porosity Determinations by Physisorption*, Elsevier, 2006. 1–27 (Chapter 1).
- [35] H. Rojas, G. Borda, P. Reyes, M. Brijaldo, J. Valencia, *J. Chil. Chem. Soc.* 56 (2011) 793.
- [36] A. Hasaninejad, M. Shekouhy, N. Golzar, A. Zare, M.M. Doroodmand, *Appl. Catal. A Gen.* 402 (2011) 11.
- [37] S. Sobhani, A. Hasaninejad, M.F. Maleki, Z.P. Parizi, *Synth. Commun.* 42 (2012) 2245.
- [38] Z. Karimi-Jaberi, B. Pooladian, M. Moradi, E. Ghasemi, *Chin. J. Catal.* 33 (2012) 1945.